Supplementary information

Kinetics and mechanism of amino acid derived 2-thiohydanoin formation reactions

Petar Stanić, Biljana Šmit, Dejan Milenković

Institute for Information Technologies, University of Kragujevac, Jovana Cvijića bb, 34000 Kragujevac, Serbia

Table S1. *Relative integral value ratios of ^{1}H NMR signals of methoxy protons of starting amino acid methyl esters at 3.72-3.73 ppm and methoxy protons of methanol at 3.45 ppm that forms during the reactions (amino acid-OCH_3/MeOH) and elapsed time for each spectrum.*

Gly		Ala		Val		Leu		Phe	
int. ratios	*t* / s	int. ratios	*t* / s	int. ratios	*t* / s	int. ratios	*t* / s	int. ratios	*t* / s
98.48/1.52	942	97.26/2.74	519	97.74/2.26	584	98.43/1.57	587	98.27/1.73	385
98.43/1.57	1114	97.03/2.97	691	97.24/2.76	756	98.27/1.23	759	97.38/2.62	557
96.71/3.29	1286	96.88/3.12	863	96.98/3.02	928	98.16/1.84	931	96.02/3.98	729
95.52/4.48	1458	96.57/3.43	1035	96.84/3.16	1100	97.50/2.50	1103	94.65/5.35	901
93.97/6.03	1930	96.18/3.82	1207	96.14/3.86	1272	97.17/2.83	1275	93.23/6.77	1073
91.84/8.16	2402	95.63/4.37	1379	95.70/4.30	1444	96.53/3.447	1447	91.46/8.54	1245
91.21/8.79	2874	93.67/6.33	1551	93.75/6.25	1616	95.62/4.38	1919	86.38/13.62	1417
88.89/11.11	3646	91.47/8.53	2023	93.16/6.84	2088	93.99/6.01	2391	80.36/19.64	1889
87.49/12.51	4418	89.01/10.99	2495	91.99/8.01	2560	91.67/8.33	2863	74.29/25.71	2361
83.46/16.54	5190	84.72/15.28	2967	89.45/10.55	3032	88.73/11.27	3635	64.32/35.68	2833
82.97/17.03	6262	80.72/19.28	3739	86.76/13.24	3804	85.38/14.62	4407	54.93/45.07	3605
78.47/21.53	7334	76.52/23.48	4511	83.96/16.04	4576	79.52/20.48	5179	46.20/53.80	4377
72.75/27.25	8406	71.10/28.90	5283	81.24/18.76	5348	75.44/24.56	6251	35.94/64.06	5149
71.49/28.51	10378	66.41/33.59	6355	76.26/23.74	6420	71.30/28.70	7323	27.47/72.53	6221
68.34/31.66	12350	61.94/38.06	7427	72.16/27.84	7492	63.07/36.93	8395	20.97/79.03	7293
59.82/40.18	14322	54.68/45.32	8499	65.64/34.36	8564	55.43/44.57	10367	13.32/86.68	8365
53.77/46.23	18094	48.76/51.24	10471	59.59/40.41	10536	49.69/50.31	12339	8.02/91.98	10337
48.85/51.15	21866	44.11/55.89	12443	54.03/45.97	12508	39.58/60.12	14311	5.07/94.93	12309
44.47/55.53	25638	35.19/64.81	14415	44.93/55.07	14480	32.93/67.07	18083	2.35/97.65	14281
40.84/59.16	29410	28.80/71.20	18187	37.59/62.41	18252	27.72/72.28	21855	1.25/98.75	18053
36.46/63.54	33182	24.36/75.64	21959	31.38/68.62	22024	23.61/76.39	25627	0.74/99.26	21825
33.22/66.78	36954	20.70/79.30	25731	26.69/73.31	25796	20.22/79.78	29399	0.73/99.27	25597
30.54/69.46	40726	17.11/82.89	29503	22.30/77.70	29568	18.70/81.30	33171		
28.18/71.82	44498	14.09/85.91	33275	18.59/81.41	33340	17.18/82.82	36943		
26.04/73.96	48270	11.84/88.16	37047	16.06/83.94	37112	14.34/85.66	40715		
22.55/77.45	52042	10.48/89.52	40819	14.52/85.48	40884	11.62/88.38	44487		
		9.15/90.85	44591	11.76/88.24	44656	10.94/89.06	48259		
		7.68/92.32	48363	10.46/89.54	48428	10.35/89.65	52031		
		6.89/93.11	52135	9.87/90.13	52200				

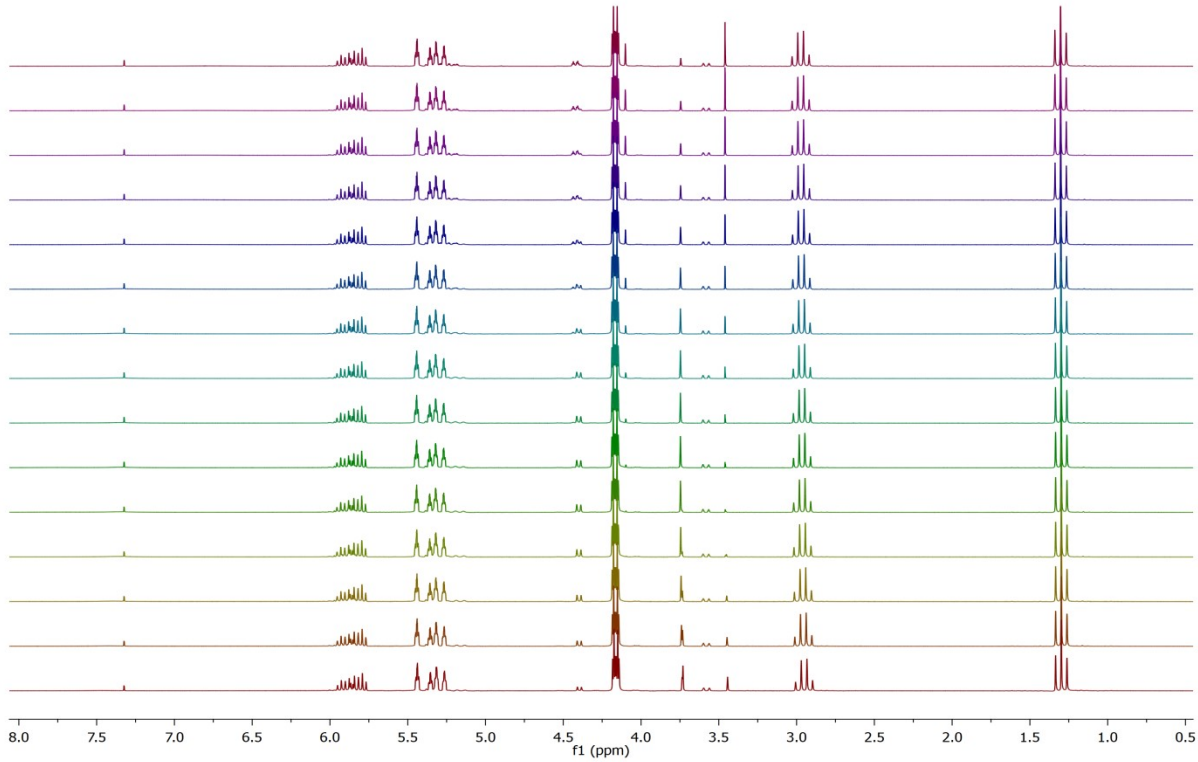

Figure S1. *^{1}H NMR spectra of the reaction of glycine methyl ester and AITC*

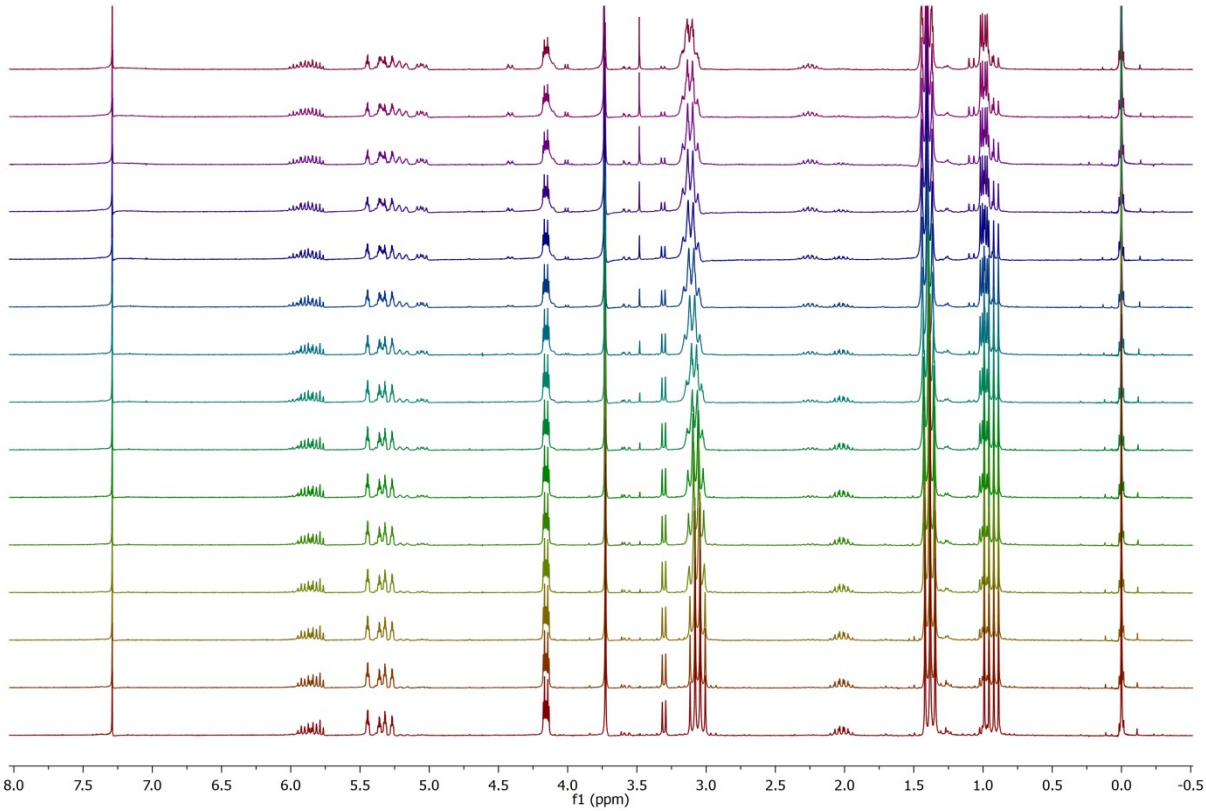

Figure S2. *^{1}H NMR spectra of the reaction of L-valine methyl ester and AITC*

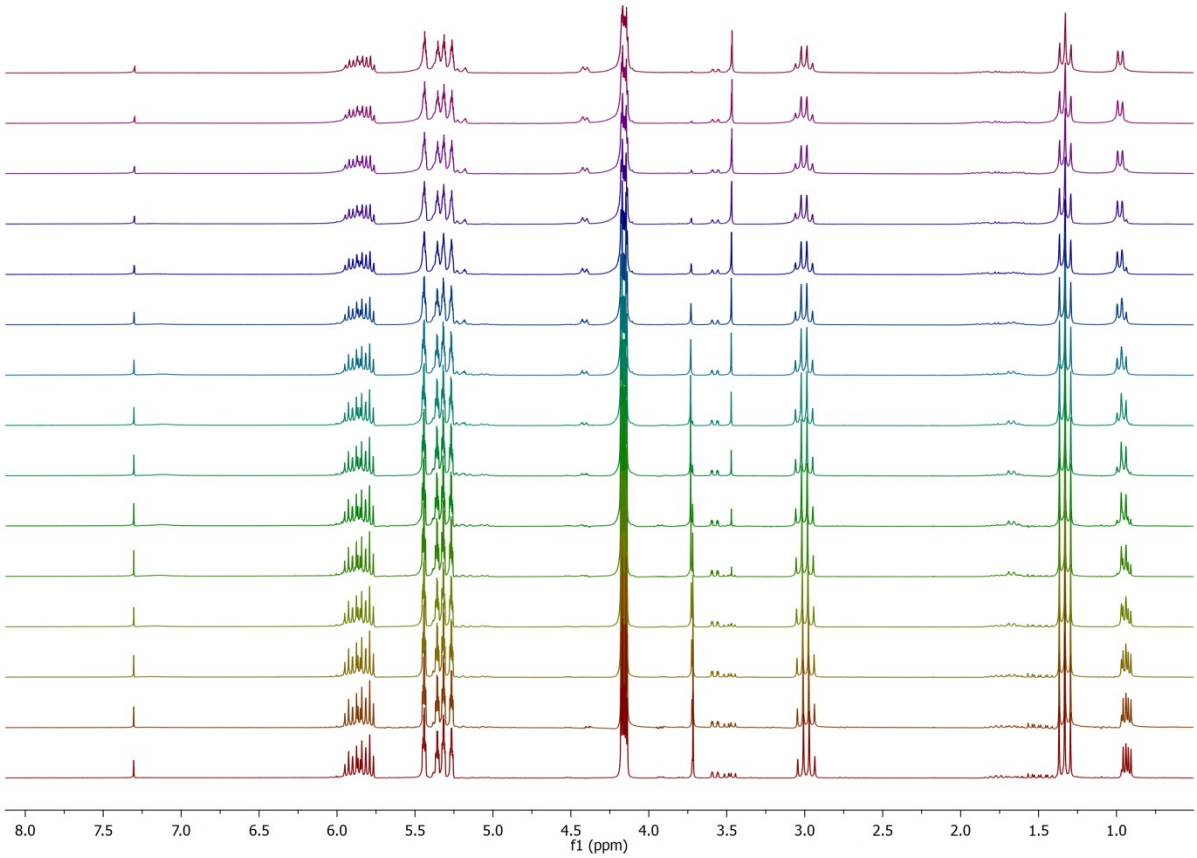

Figure S3. *^{1}H NMR spectra of the reaction of L-leucine methyl ester and AITC*

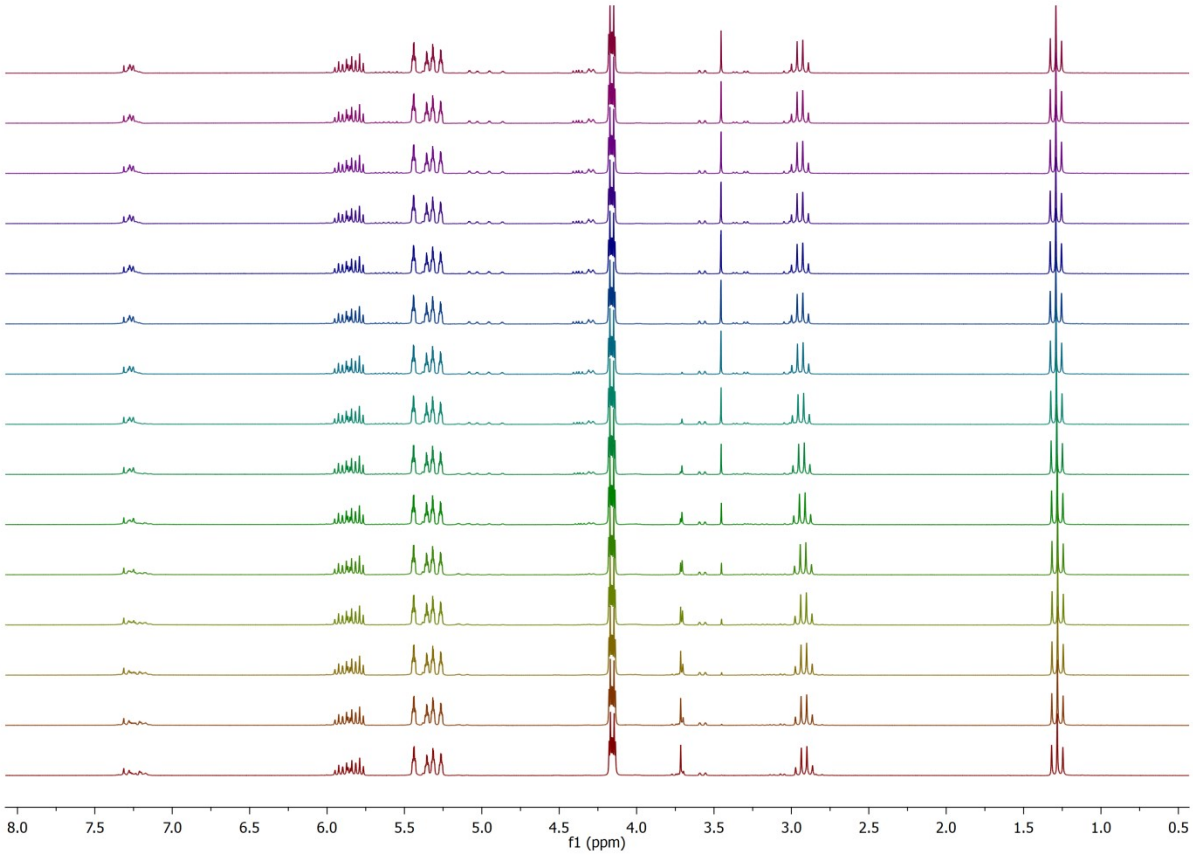

Figure S4. *^{1}H NMR spectra of the reaction of L-phenylalanine methyl ester and AITC*

Glycine methyl ester hydrochloride. White solid. ^{1}H NMR (200 MHz, D_2O) δ 3.85 (s, 3H), 3.94 (s, 2H) ppm.
Alanine methyl ester hydrochloride. White solid. ^{1}H NMR (200 MHz, D_2O) δ 1.52 (m, 3H), 3.79 (s, 3H), 4.15 (m, 1H) ppm.

Valine methyl ester hydrochloride. White solid. ^{1}H NMR (200 MHz, D_2O) δ 1.15 (dd, J = 2.6 and 7.0 Hz, 6H), 2.47 (m, 1H), 3.83 (s, 3H), 3.98 (d, J = 4.4 Hz, 1H) ppm.

Leucine methyl ester hydrochloride. White solid. ^{1}H NMR (200 MHz, D_2O) δ 0.96 (d, J = 6.2 Hz, 6H), 1.79 (m, 3H), 3.84 (s, 3H), 4.15 (dd, J = 5.8 and 7.6 Hz, 1H) ppm.

Phenylalanine methyl ester hydrochloride. White solid. ^{1}H NMR (200 MHz, D_2O) δ 3.26-3.35 (m, 2H) 3.85 (s, 3H), 4.44 (t, 1H), 7.30 (m, 2H), 7.42-7.45 (m, 3H) ppm.

3-Allyl-2-thioxoimidazolidin-4-one. Brownish-yellow rod-like crystals; IR (KBr) ν_{max}: 3225, 2923, 1751, 1650, 1526, 1430, 1343, 1259, 1173, 929, 697 cm^{-1}; ^{1}H NMR (200 MHz, CDCl3) δ 4.17 (d, J = 1.4 Hz, 2H), 4.37 (dt, J = 1.2 and 6.0 Hz, 2H), 4.99–5.35 (m, 2H), 5.74–5.97 (m, 1H), 7.78 (bs, 1H) ppm; ^{13}C NMR (50 MHz, CDCl3) δ 43.3, 48.5, 118.7, 130.5, 171.7, 184.7 ppm.

3-Allyl-5-methyl-2-thioxoimidazolidin-4-one. Yellowish needle crystals; IR (KBr) ν_{max}: 3170, 3012, 2920, 1743, 1647, 1538, 1429, 1346, 1263, 1171, 927, 636 cm^{-1}; 1H NMR (200 MHz, CDCl3) δ 1.49 (d, J = 6.8 Hz, 3H), 4.21 (q, J = 6.8 Hz, 1H), 4.43 (dt, J = 1.2 and 6.0 Hz, 2H), 5.19–5.32 (m, 2H), 5.76–5.98 (m, 1H), 7.22 (bs, 1H) ppm; 13C NMR (50 MHz, CDCl3) δ 11.0, 43.3, 55.0, 118.5, 130.6, 174.1, 183.5 ppm.

3-Allyl-5-isopropyl-2-thioxoimidazolidin-4-one. Yellowish needle crystals; IR (KBr) ν_{max}: 3292, 3093, 2963, 1725, 1648, 1512, 1428, 1355, 1254, 1171, 929, 664 cm^{-1}; ^{1}H NMR (200 MHz, CDCl3) δ 0.94 (d, J = 6.8 Hz, 3H), 1.08 (d, J = 6.8 Hz, 3H), 2.19–2.38 (m, 1H), 4.00 (dd, J = 1.4 and 2.0 Hz, 1H), 4.42 (d, J = 5.6 Hz, 2H), 5.18–5.32 (m, 2H), 5.73–5.96 (m, 1H), 7.61 (bs, 1H) ppm; ^{13}C NMR (50 MHz, CDCl3) δ 16.3, 18.8, 30.9, 43.1, 64.6, 118.5, 130.6, 173.1, 184.0 ppm.

3-Allyl-5-isobutyl-2-thioxoimidazolidin-4-one. White tiny needle crystals; IR (KBr) ν_{max}: 3181, 3006, 2956, 1754, 1650, 1534, 1433, 1346, 1253, 1175, 926, 656 cm^{-1}; ^{1}H NMR (200 MHz, CDCl3) δ 0.98 (d, J = 6.0 Hz, 3H), 1.52–1.90 (m, 3H), 4.14 (dd, J = 2.6 and 9.6 Hz, 1H), 4.42 (dt, J = 1.2 and 5.6 Hz, 2H), 5.19–5.30 (m, 2H), 5.75–5.97 (m, 1H), 7.78 (bs, 1H) ppm; ^{13}C NMR (50 MHz, CDCl3) δ 21.5, 23.0, 25.2, 40.4, 43.2, 58.0, 118.4, 130.5, 174.0, 183.5 ppm.

3-Allyl-5-benzyl-2-thioxoimidazolidin-4-one. White tiny needle crystals; IR (KBr) ν_{max}: 3205, 3033, 2920, 1749, 1647, 1524, 1428, 1344, 1250, 1175, 931, 732, 651 cm^{-1}; ^{1}H NMR (200 MHz, CDCl3) δ 2.89 (dd, J = 9.0 and 14.0 Hz, 1H), 3.33 (dd, J = 3.6 and 14.0 Hz, 1H), 4.32 (m, J = 3.8 Hz, 1H), 4.36 (dd, J = 1.6 and 5.6 Hz, 2H), 5.01–5.19 (m, 2H), 5.61–5.82 (m, 1H), 7.18–7.40 (m, 6H) ppm; ^{13}C NMR (50 MHz, CDCl3) δ 37.6, 43.2, 60.4, 118.4, 127.7, 129.1, 130.4, 134.6, 172.7, 183.5 ppm.

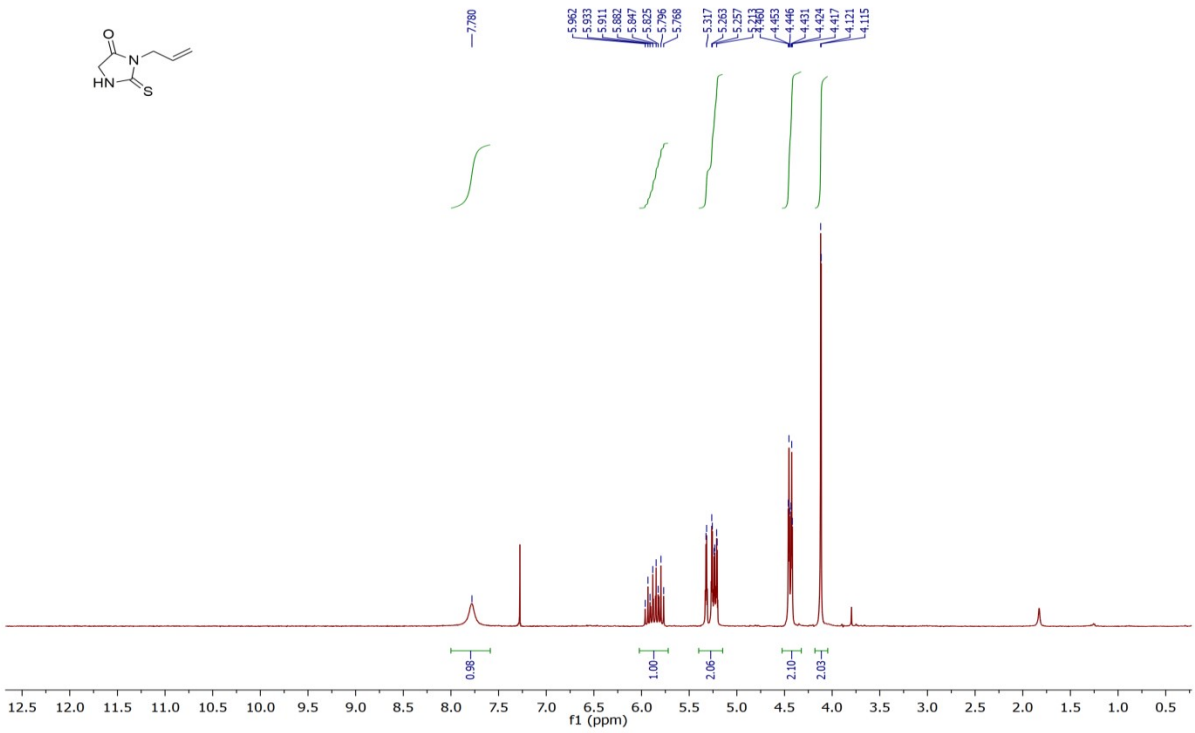

Figure S5. *[1]H NMR spectra of 3-allyl-2-thioxoimidazolidin-4-one.*

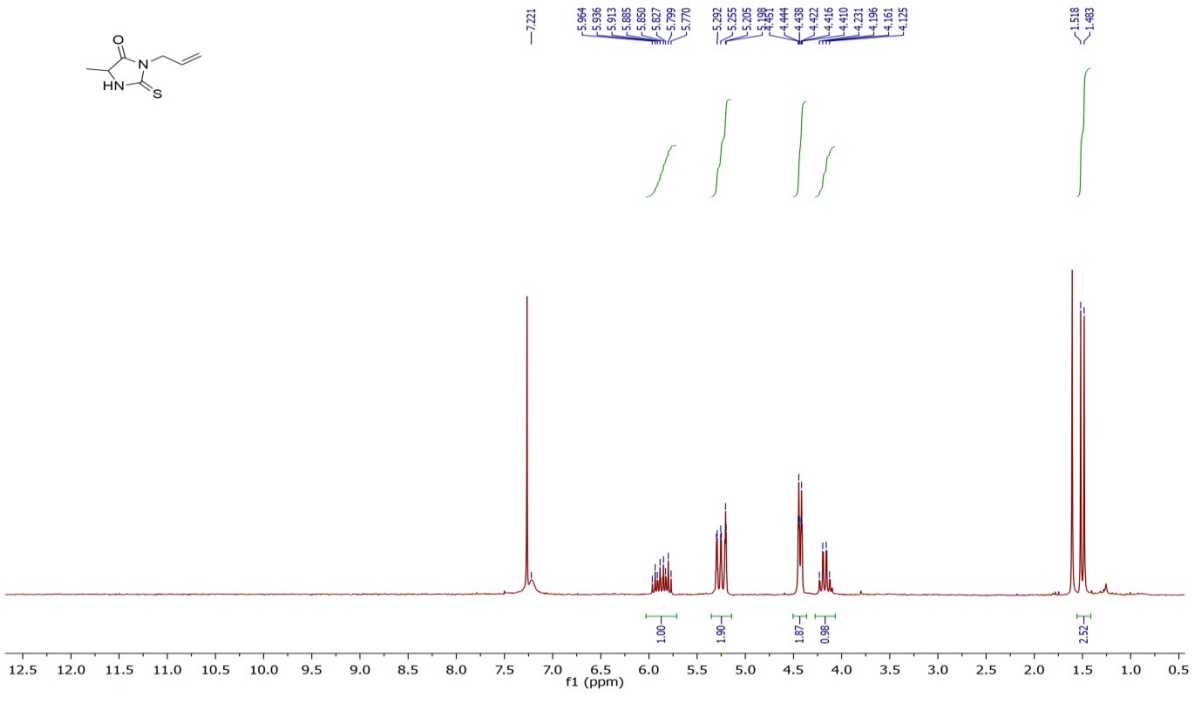

Figure S6. *[1]H NMR spectra of 3-allyl-5-methyl-2-thioxoimidazolidin-4-one.*

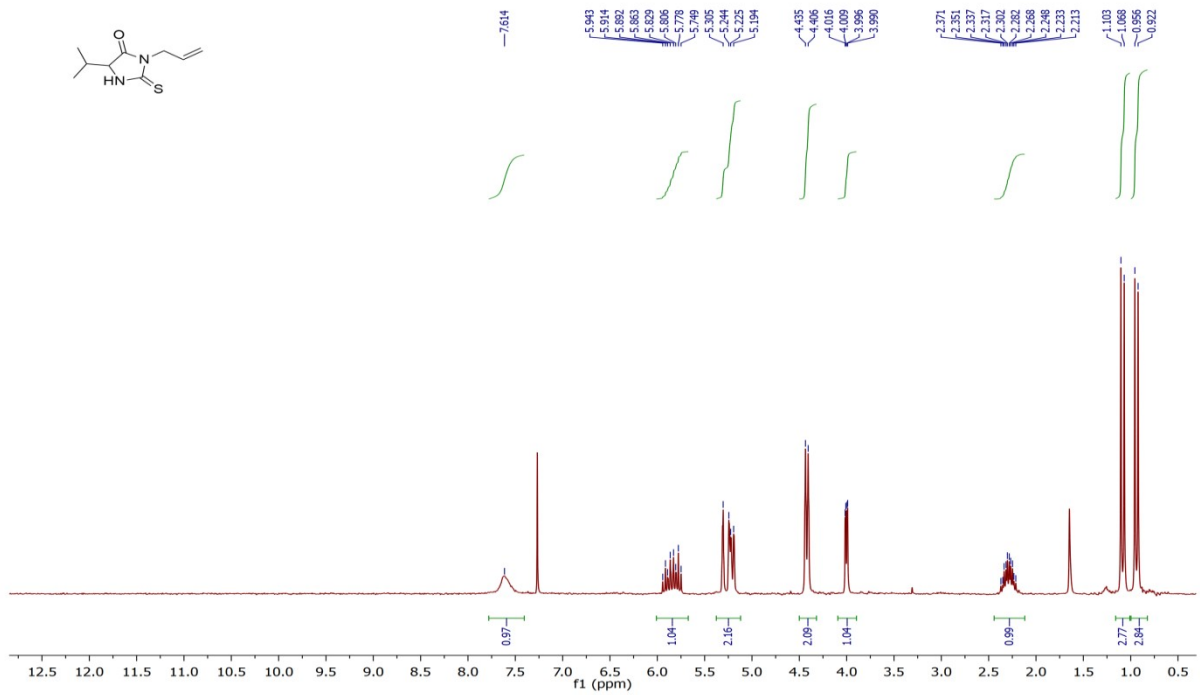

Figure S7. *[1]H NMR spectra of 3-allyl-5-isopropyl-2-thioxoimidazolidin-4-one.*

.

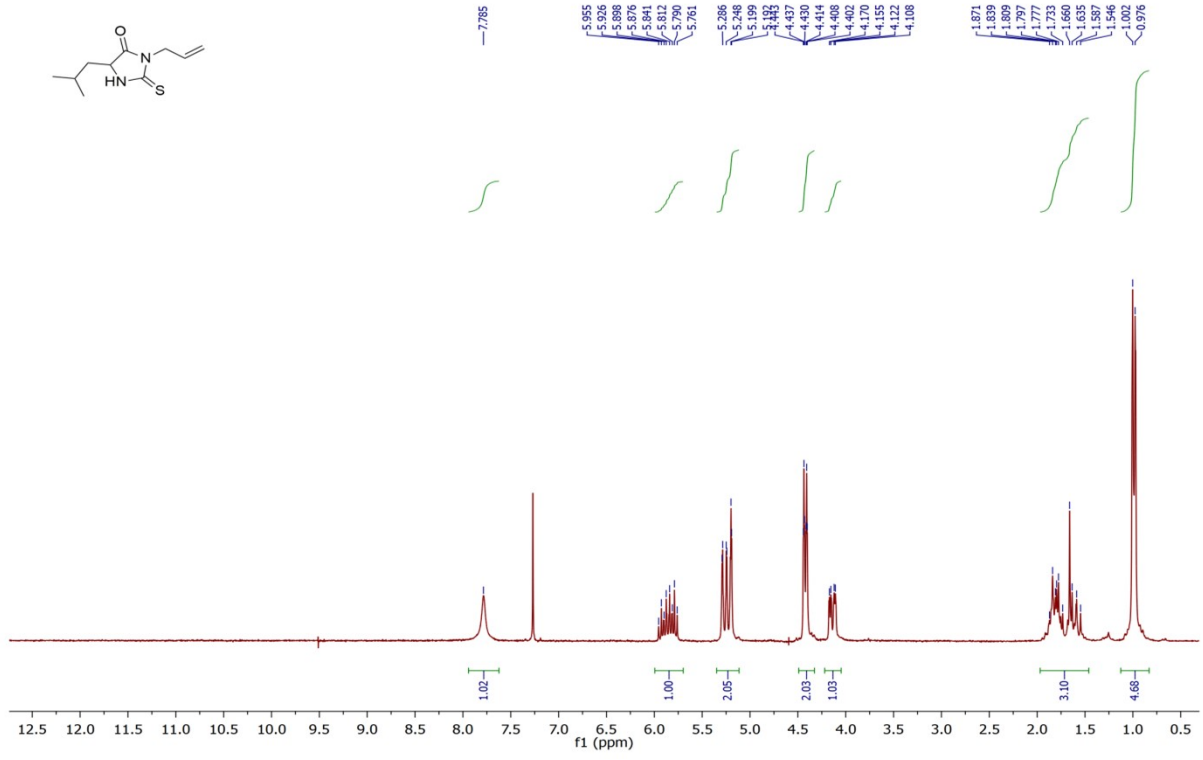

Figure S8. *[1]H NMR spectra of 3-allyl-5-isobutyl-2-thioxoimidazolidin-4-one.*

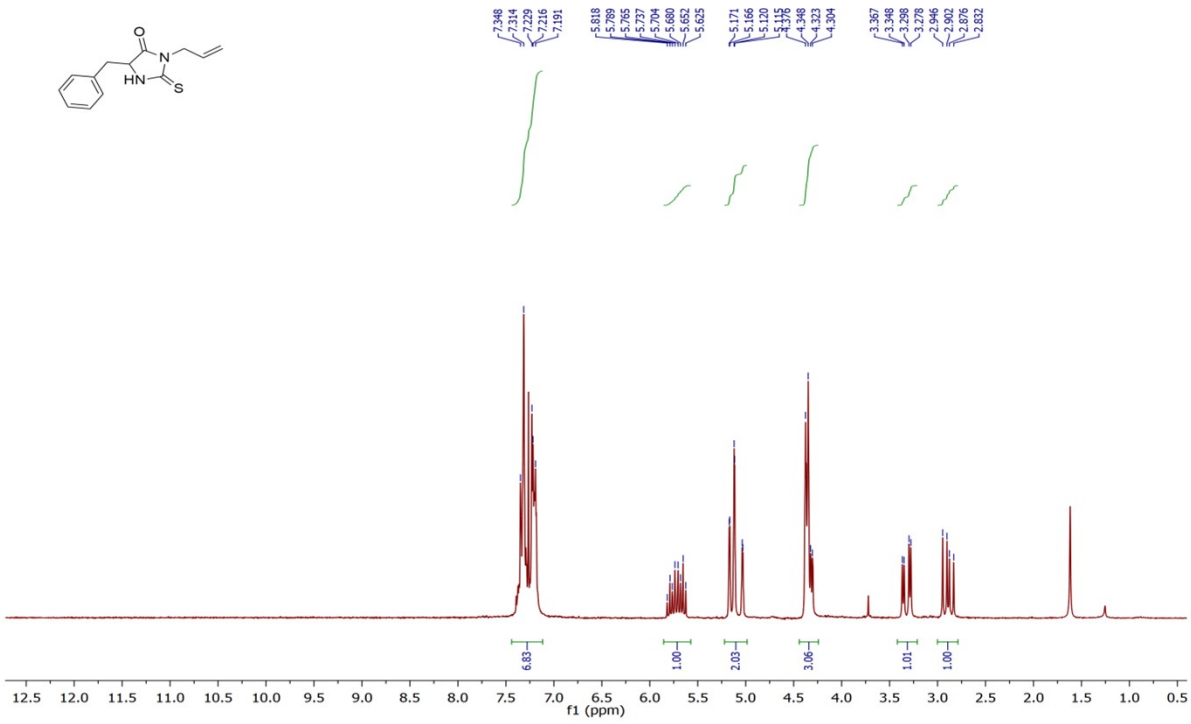

Figure S9. *^{1}H NMR spectra of 3-allyl-5-benzyl-2-thioxoimidazolidin-4-one.*

NBO analysis

The electronic structure of product, **5-ala** was examined using the NBO analysis. In order to evaluate the donor–acceptor interactions, the analysis of the second order Fock matrix was performed. The stabilization energy ($E^{(2)}$) for each donor (i) and acceptor (j) associated with the delocalization between i and j, is determined as:

$$E^{(2)} = \Delta E_{ij} = q_i \frac{(F_{ij})^2}{\left(E_j - E_i\right)}$$

where q_i is the donor orbital occupancy, E_i, E_j are the diagonal elements (orbital energies) and $F_{i,j}$ is the off diagonal NBO Fock matrix element. The large $E^{(2)}$ value indicates the intensive interaction between the electron-donors and electron-acceptors and greater extent of conjugation of the whole system. The possible intensive interactions are given in Table S2.

Table S2. *Second order perturbation theory analysis of* ***5-ala*** *Fock matrix.*

Donor(i)	Acceptor(j)	ED(i)	ED(j)	$E^{(2)}$ / kJ mol^{-1}	E_i–E_j / a.u.	$F_{i,j}$ / a.u.
LP2 O4	σ*C5-C4	1.86	0.08	93.7	0.78	0.12
LP2 O4	σ*C4-O4	1.86	0.09	157.0	0.80	0.16
LP1 OCH_3	σ*C4-OCH_3	1.96	0.02	37.4	1.36	0.10
LP1 OCH_3	σ*N3-H3	1.96	0.03	17.5	1.15	0.062
LP2 OCH_3	π*C4-O4	1.80	0.20	245.7	0.47	0.15
LP1 N1	σ*C5-C4	1.71	0.08	43.1	0.73	0.08
LP1 N1	σ*C2-S	1.71	0.53	393.0	0.26	0.15
LP2 S	σ*N1-C2	1.90	0.05	50.5	0.77	0.09
LP2 S	σ*C2-N3	1.90	0.06	56.5	0.79	0.09
LP1 N3	σ*C2-S	1.68	0.53	461.5	0.26	0.16

The most important interaction (n-σ*) energies, related to the delocalization in the molecule, are electron donation from the LP1 N atom orbitals to the anti-bonding acceptor σ *(C–S) (LP1 N3 and LP1 N1 → σ*C2-S). These interactions lead to an increase in electron density (ED) in the C-S anti-bonding orbital, which weakens their respective bonds. The ED at the nitrogen atoms N3 and N1 (1.68 to 1.71 e) and at the σ* bonds (0.53 e) of the C-S clearly demonstrate strong electron delocalization, leading to the stabilization by ~393– 462 kJ mol^{-1}. Also, the other LP2 O lone electron pairs show a significant electron donating ability to the anti-bonding acceptor π*(C–O), σ* (C–O) and σ* (C–C) orbitals.

The **5-ala** structure is characterized by one intramolecular hydrogen bond (IHB) which additionally stabilizes the structure. The strong hydrogen bond (2.08 Å) is formed between N3-H3 and O from methoxy group. This result is expected since it is well known that the NH groups are good hydrogen bond donors. The NBO analysis revealed that the electron density is donated from the *p* orbital of oxygen from methoxy group into the proximate σ*(N3-H3) bond. This hydrogen bond additionally stabilizes the structure with energy of 17.5 kJ mol^{-1}.

The N3–C2 and N1–C2 bond lengths of about 1.342 and 1.359 Å lie between the bond lengths characteristic to the double C=N and single C–N bonds indicating the partial double character of these bonds which enable the electron delocalization in **5-ala**. This assumption is supported by the NBO analysis. A slightly greater *p*-orbital contribution on C2 in N3–C2 and N1–C2 bonds (hybrid compositions 0.788($sp^{1.63}$)N3 + 0.616($sp^{2.10}$)C2 and 0.788($sp^{1.62}$)N1 +

0.616($sp^{2.17}$)C2) could be the main reason for this bond being slightly longer than a double C=N bond.

QTAIM analysis

QTAIM analysis also shown that bond critical points (BCP) of N3-H3---O-CH_3 hydrogen bond have the values for electron density and Laplacian: 0.191 eA and 0.077 a.u. These parameters indicate that this bond is strong hydrogen bond because the value of density is above the common values for hydrogen bond, but still below covalent bonds, while the value of Laplacian is positive.

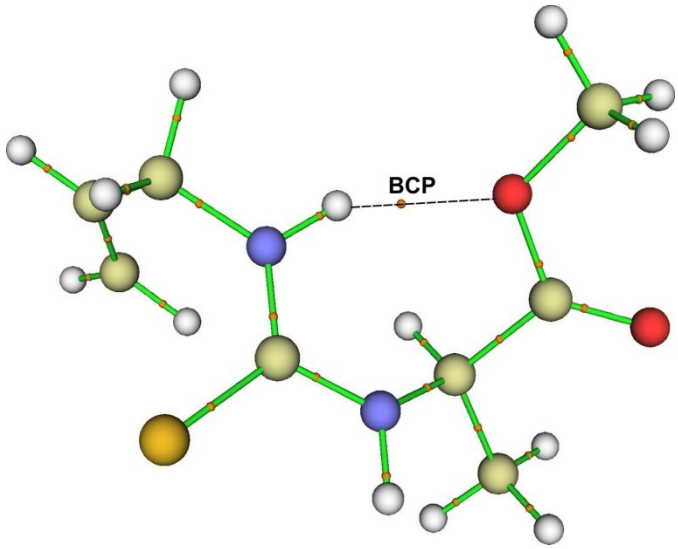

Figure S10. *Bond critical points (BCP) of product,* ***5-ala***.

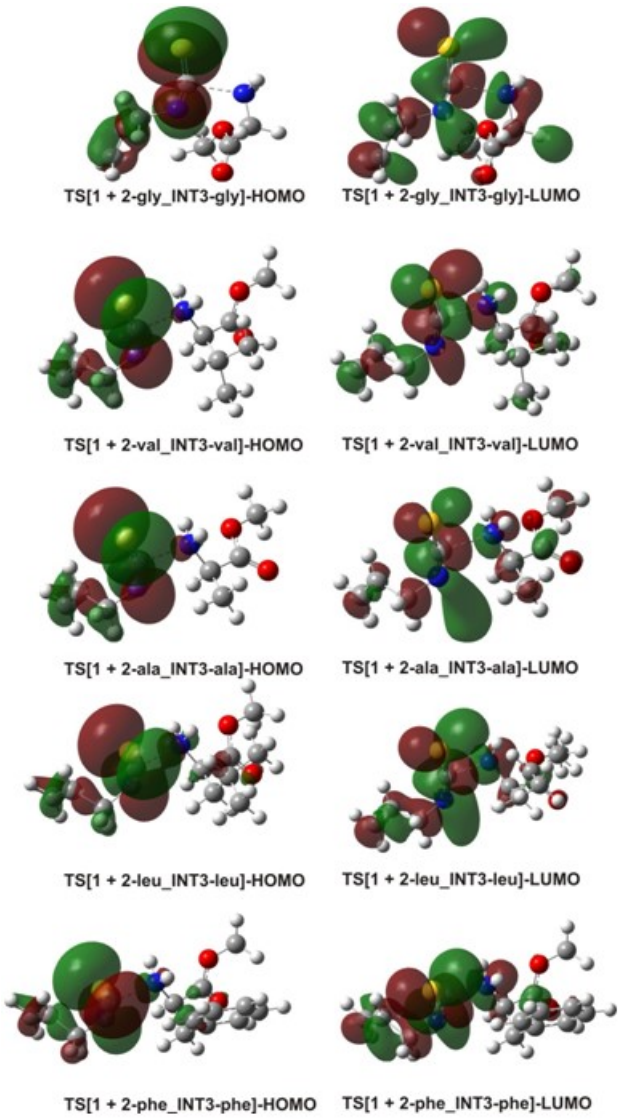

Figure S11. *The shape of HOMO and LUMO in TSs for the reaction between L-alanine methyl ester and AITC.*

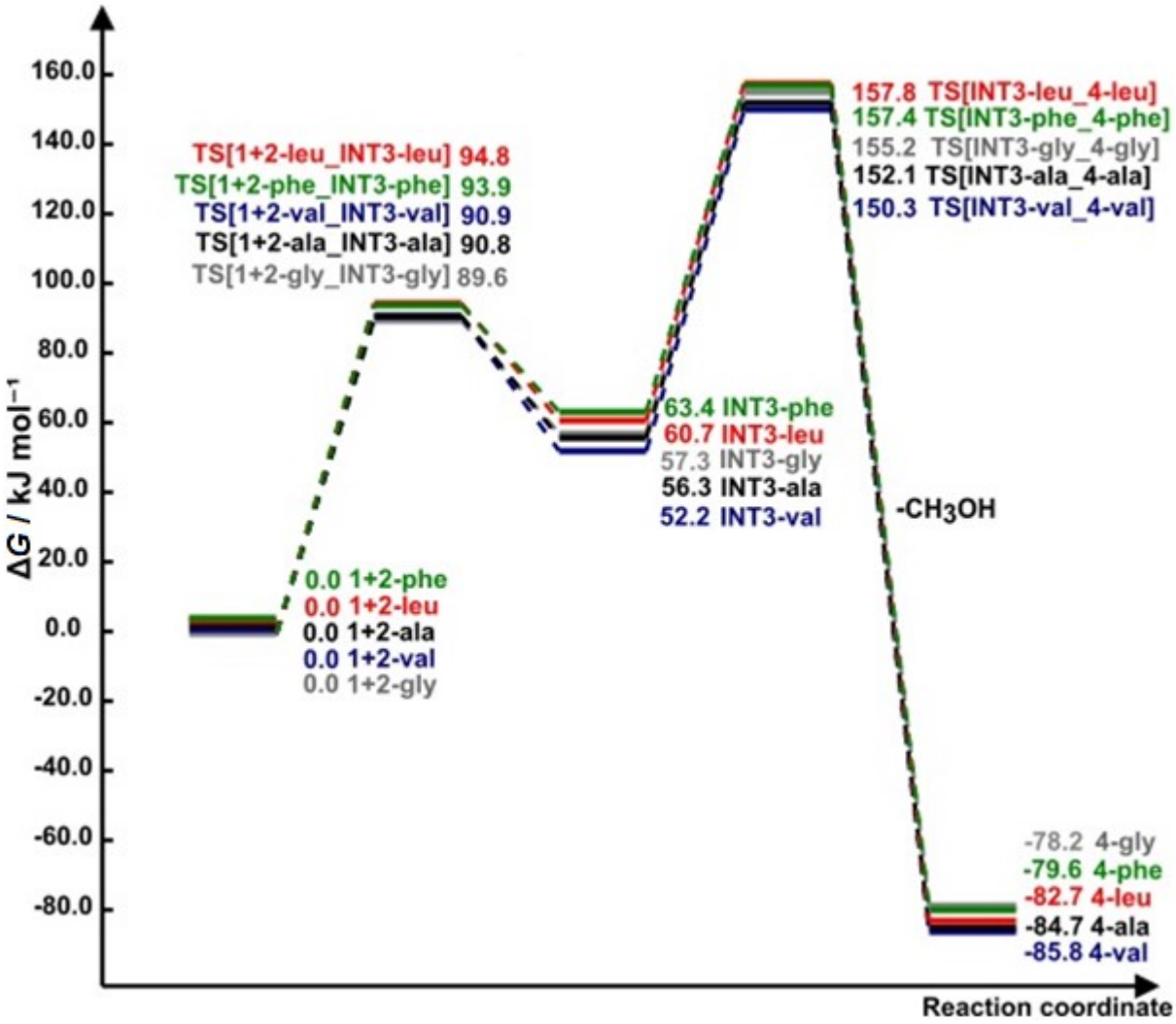

Figure 12. *Free energy profile for the* ***1 + 2 → INT3 → 4*** *reaction path.*

Table S3. *Bond critical point parameters for C2-N1 bond in all TSs of the addition step; ρ(r) is electron density, ∇²ρ is Laplacian of electron density, G(r) and V(r) are kinetic and potential electron densities; N1 is the nucleophilic nitrogen from the amino acid methyl ester, C2 is the electrophilic carbon from AITC.*

BCP for C2-N1 bond	ρ(r)	$\nabla^2\rho$	V(r)	G(r)
TS[1+2-gly_INT3-gly]	0.056	0.091	-0.040	0.031
TS[1+2-val_INT3-val]	0.055	0.090	-0.039	0.030
TS[1+2-ala_INT3-ala]	0.054	0.090	-0.038	0.031
TS[1+2-leu_INT3-leu]	0.055	0.090	-0.039	0.030
TS[1+2-phe_INT3-phe]	0.055	0.090	-0.039	0.030